Reprinted from Optics Letters, Vol. 13, page 589, July 1988.

Self-focusing and self-phase modulation in a parabolic graded-index optical fiber

Jamal T. Manassah, P. L. Baldeck, and R. R. Alfano

Department of Electrical Engineering, The City College of New York, New York, New York 10031

Received January 13, 1988; accepted April 24, 1988

The spatial profile and the spectral distribution of a pulse propagating in a parabolic graded-index optical fiber are derived. Effects due to the $\chi^{(3)}$ nonlinearity (self-focusing and self-phase modulation), diffraction (finite beam-waist effects), and the graded-index waveguiding are incorporated in the theoretical analysis. The fiber graded index generates a periodicity in the beam diameter. Waveguiding, self-focusing, and diffraction determine the minimum magnitude of the beam-waist diameter. The pulse phase, amplitude shape, and spectral distribution are shown to differ from conventional self-phase modulation results.

Over the years, self-focusing of intense pulses has been observed in many liquids and solids.[1–4] Kelley theoretically described the self-focusing process in terms of critical power.[2] The propagation of Gaussian beams in a graded-index waveguide structure leads to the appearance of a sequence of maxima and minima in the field intensity along the length of the fiber.[5] The first observation of self-focusing in optical fibers by using picosecond pulses has been reported recently.[6]

In this Letter, we examine the combined effects of the Kerr nonlinearity, diffraction, and graded-index waveguiding on the spatial and spectral profiles of an intense pulse propagating in a parabolic graded-index optical fiber. The beam transverse geometrical shape, radius of curvature, phase, and spectrum are computed as functions of the fiber parameters and the pulse peak power. Approximate analytical results are derived for the beam waist, radius of curvature, and phase.

The approximations that we make are that (1) the graded-index profile is approximated by[7] $n = n_0(1 - Ar^2/2n_0)$; (2) the fiber core–cladding boundary conditions are neglected, assuming that the beam diameter a is much smaller than the core radius r_c; (3) effects of group-velocity dispersion are neglected; (4) the self-steepening[8,9] of the amplitude is neglected, which in the notation of Ref. 8 translates into $\epsilon V < 0.1$; (5) the quadratic index of refraction n_2 is not modified by the radial variation in the ordinary index of refraction; (6) one component of the electric field is kept, i.e., we are neglecting the vector nature of the electric field; and (7) the graded index of refraction is of the order required to guide[7] the beam. Under these assumptions the envelope of the electric field, ϵ, obeys the equation

$$\nabla_T^2\epsilon - 2ik\epsilon' - kk_2r^2\epsilon + \frac{n_2k^2}{n_0}|\epsilon|^2\epsilon = 0, \tag{1}$$

where ∇_T^2 is the transverse component of the Laplacian, $\epsilon' = \partial\epsilon/\partial z$, $k_2 = kA = 2kn_0\Delta/r_c^2$, and Δ is the relative index difference between the core center and the cladding.

The initial pulse is assumed to be Gaussian both in the transverse plane and in the comoving coordinate system $u = (z/v_g - t)$, where v_g is the pulse group velocity, a is the initial beam radius, τ is the pulse duration, and ϵ_0 is the magnitude of the pulse amplitude. This initial condition assumes that the beam radius is much smaller than the core radius.

Below, the product $\epsilon_0 \exp(-u^2/2\tau^2)$ is denoted by $\tilde{\epsilon}_0$. Then an approximate solution to Eq. (1), with the above boundary condition, correct to order r^2/a^2, can be obtained through the trial solution[9]:

$$\epsilon(r, z, u) = \frac{\tilde{\epsilon}_0}{\omega(z, u)} \exp\left[-\frac{r^2}{a^2\omega^2(z, u)} - i\frac{k}{2}\rho(z, u)r^2 + ik\alpha(z, u)\right], \tag{2}$$

where the different functions can be interpreted as follows: ω is the normalized beam radius, ρ is the inverse of the beam radius of curvature, and $k\alpha$ is the longitudinal phase on the fiber axis. This approximation of self-similarity of the beam is well justified for powers smaller than the critical power, in particular for instances where $\omega_{\max}$ and $\omega_{\min}$ are not too far apart.

The equations satisfied by these subsidiary functions are

$$\rho = \frac{1}{\omega}\frac{\partial\omega}{\partial z}, \tag{3}$$

$$\frac{\partial\alpha}{\partial z} = \frac{a^2}{2\omega^2}(B - C), \tag{4}$$

$$\frac{\partial^2\omega}{\partial z^2} + A\omega + (2C - B)\frac{1}{\omega^3} = 0, \tag{5}$$

where $A = 1/L_w^2$, $B = 4/a^4k^2 = 1/L_d^2$, $C = n_2\tilde{\epsilon}_0^2/n_0a^2$, and L_w and L_d are the characteristic lengths for waveguiding and diffraction, respectively.

The solutions to Eqs. (4)–(6), satisfying the boundary conditions $\omega = 1$, $\rho = 0$, and $\alpha = 0$ at $z = 0$, are

$$\omega = [\beta\cos(\gamma z) + \delta]^{1/2}, \tag{6}$$

0146-9592/88/070589-03$02.00/0

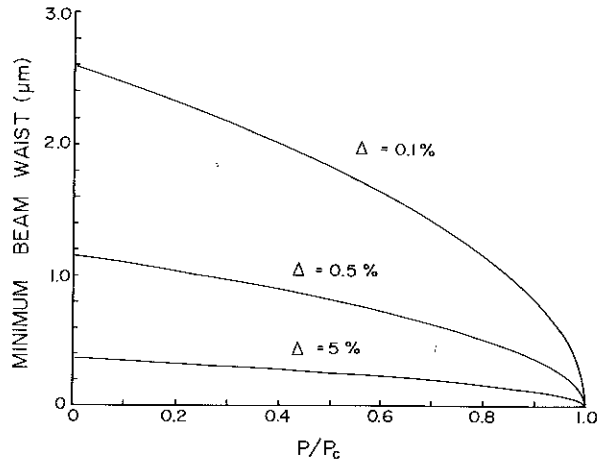

Fig. 1. Minimum beam waist as a function of normalized peak power P/P_c. Δ is the relative refraction index difference between the core center and the cladding. In silica fibers $P_c \approx 10^6$ W.

$$\rho = -\frac{1}{2}\frac{\beta\gamma \sin(\gamma z)}{[\beta \cos(\gamma z) + \delta]}, \tag{7}$$

$$k\alpha = k\frac{a^2(B-C)}{2(B-2C)^{1/2}} \arctan\left[\left(\frac{B-2C}{A}\right)^{1/2} \tan(A^{1/2}z)\right], \tag{8}$$

where $\gamma = 2A^{1/2}$, $\beta = (2C - B + A)/2A$, and $\delta = (A - 2C + B)/2A$. The above solutions are valid for $\beta \leq \delta$ or, equivalently, $B - 2C \geq 0$. For negative n_2 (defocusing medium), $\beta < \delta$ is satisfied for all values of ϵ. For positive n_2 (focusing medium), $\beta = \delta$ for the critical field ϵ_c, which is given by $\epsilon_c^2 = 2n_0/a^2k^2n_2$. In the low-intensity limit, Eqs. (6)–(8) lead to the usual results of Gaussian beams propagating in lenslike media.[10,11]

Equation (6) shows that the normalized beam radius ω varies periodically along the optical fiber length. The period of variation depends only on the waveguiding characteristic length L_w. The magnitude of $\omega_{\min}$, the minimum normalized beam waist, depends on all three characteristic lengths. In Fig. 1, the minimum beam waist is plotted as a function of the pulse-normalized peak power P/P_c for different graded-index parameters Δ, where P_c is the critical power for self-focusing. The minimum beam diameter decreases for increasing peak powers and collapses at $P = P_c$.

The inverse of the radius of curvature (ρ) is plotted in Fig. 2 as a function of the normalized fiber length $2z/(\pi L_w)$. For increasing peak powers, the curvature is clearly enhanced periodically by self-focusing at the beam-waist locations.

The total phase of the electric field can be computed by using Eqs. (2), (7), and (8). This phase, and consequently the spectral broadening arising from self-phase modulation, is radially dependent. It is worth noting that the time-dependent part of the phase ϕ' (denoted ϕ_t', equal to total phase $- \omega_0 t$), reduces to that of the traditional self-phase-modulation theory in the case of a homogeneous medium ($k_2 = 0$) and for an incoming plane wave ($a \to \infty$). Furthermore, for weak waveguiding ($k_2 \to 0$) but finite initial beam diameter, the time-dependent phase ϕ_t' reduces to

$$\lim_{k_2 \to 0} \phi_{t'} = \phi_{\text{spm}}\left(1 - \frac{2r^2}{a^2}\right), \tag{9}$$

where ϕ_{spm} is $-(kn_2/2n_0)\tilde{\epsilon}_0^2 z$. Thus in this limit the spectral extent as a function of the radius varies as $(1 - 2r^2/a^2)$. Equation (9) is valid for $r/a \ll 1$.

In Fig. 3, the longitudinal phase contribution $k\alpha(z, u = 0)$, denoted α phase, is plotted as a function of the normalized fiber length for different power levels. As shown, the α phase mostly increases by steps at z locations corresponding to the periodical positions of the minimum beam waist. As a result, the total amount of the longitudinal phase yielded by the pulse is often much larger than the usual self-phase modulation, and it depends strongly on the waveguiding, diffraction, and nonlinear parameters. It is worth noting that for $z \ll L_w$ the regularized α phase, defined as the value of the α phase at a certain power minus its value for zero intensity, has the same sign as ϕ_{spm}; however, this sign changes for $z > L_w$. Physically, this result

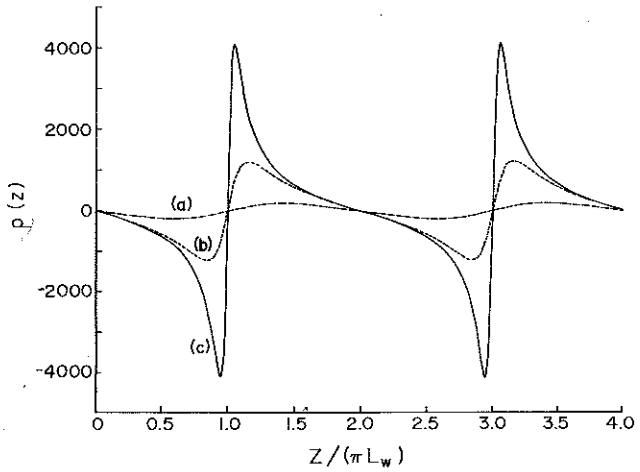

Fig. 2. Inverse of radius of curvature as a function of normalized length $2z/\pi L_w$ for a graded-index fiber ($a = 1.5$ μm, $\Delta = 0.48\%$, and $L_w = 15.3$ μm). (a) $P/P_c = 0.1$; (b) $P/P_c = 0.9$; (c) $P/P_c = 0.99$.

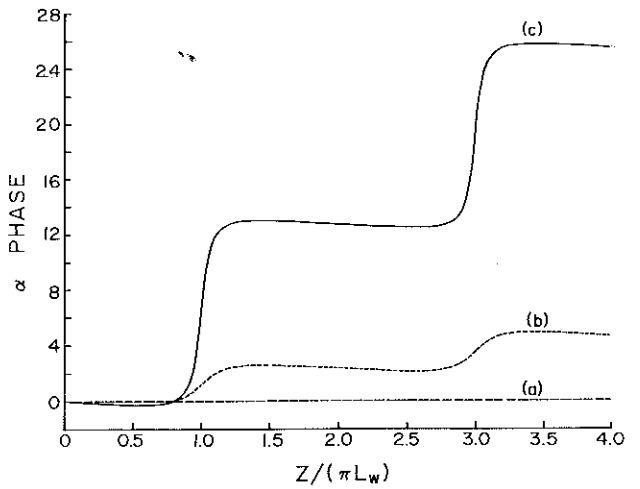

Fig. 3. α Phase as a function of the normalized length $2z/\pi L_w$. (a) $P/P_c = 0.1$; (b) $P/P_c = 0.9$; (c) $P/P_c = 0.99$.

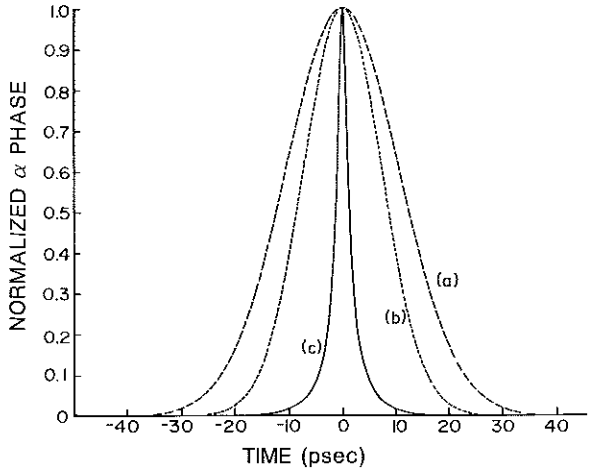

Fig. 4. α Phase normalized to its maximum value plotted versus time. (a) Conventional self-phase-modulation phase for $P/P_c = 0.1$; (b) $P/P_c = 0.1$; (c) $P/P_c = 0.992$. Maximum phases are 0.92, 0.55, and 1880 rad, respectively ($a = 25$ μm, $\Delta = 0.48\%$, $z = 10$ cm, and $\tau = 15$ psec).

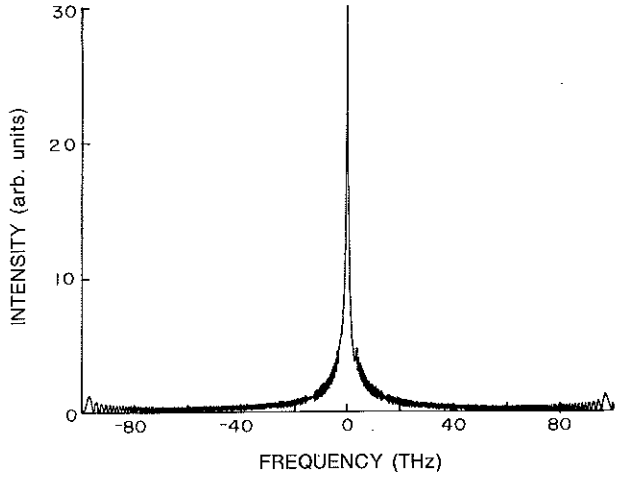

Fig. 5. Spectral broadening of a Gaussian pulse ($\tau = 15$ psec) outgoing from a graded-index fiber ($a = 25$ μm, $\Delta = 0.48\%$). $P/P_c = 0.997$ and $z = 0.1$ m.

leads to the reverse of the red leading the blue in the supercontinuum and may have important consequences on soliton propagation in graded-index fibers and pulse compression. Finally, one notices that the α phase approaches a ladder function for values of ϵ that equalize B and $2C$ (i.e., $P \to P_c$).

The temporal distribution of the longitudinal phase, the α phase, can be studied by using Eq. (9). If we define the parameter s as $C = sB[\exp(-u^2/\tau^2)]$, where $s = 1/2$ corresponds to $P = P_c$, then

$$\frac{\alpha\ \text{phase}_{\text{reg}}}{\phi_{\text{spm}}(u=0)} \approx \left(\frac{A}{B}\right)^{1/2} \frac{1}{s} \times \frac{\{[1-2s\exp(-u^2/\tau^2)]^{1/2} + s\exp(-u^2/\tau^2) - 1\}}{[1-2s\exp(-u^2/\tau^2)]^{1/2}}. \quad (10)$$

In Fig. 4, the α phase normalized to its maximum value [Eq. (10)] is plotted as function of time for different power levels. For small peak powers, the width of the phase envelope is $\sqrt{2}$ smaller than the conventional self-phase-modulation phase as predicted by Eq. (10). As the pulse peak power increases and tends to the critical power, the phase width significantly decreases and the value of the phase at its maximum increases dramatically.

The spectral distribution of intense ultrafast pulses propagating in a graded-index fiber is computed by taking the Fourier transform of the field envelope defined by Eqs. (2) and (6)–(8). For small peak powers ($P \ll P_c$) self-phase-modulation spectra generated in graded-index fibers are similar to the conventional self-phase-modulation-broadened spectra.[12] For peak powers near the critical power for self-focusing ($P \approx P_c$), new self-phase-modulation features appear (Fig. 5). Self-phase-modulation spectra in the presence of self-focusing are quite distinct from those predicted by the conventional self-phase-modulation theory. There is an intense peak at the laser wavelength over a much weaker background of white light. This supercontinuum broadening is due to the narrowing of the α phase, as observed in Fig. 4. This is because most of the pulse energy is not modulated. It is reminiscent of frequency supercontinua generated much earlier by self-focusing filaments.[3]

In conclusion, the beam transverse shape and the radius of curvature in the presence of waveguiding, self-focusing, and diffraction in a parabolic index material have been derived. The phase is qualitatively different from that predicted by the conventional self-phase modulation theory. The results in both the time domain and frequency domain are modified.

We gratefully acknowledge the partial support received from Hamamatsu Photonics K.K. We would like to thank A. Seas for his assistance in drawing the figures.

References

1. R. Y. Chiao, E. Garmire, and C. H. Townes, Phys. Rev. Lett. **13,** 479 (1964).
2. P. L. Kelley, Phys. Rev. Lett. **15,** 1085 (1965).
3. R. R. Alfano and S. L. Shapiro, Phys. Rev. Lett. **24,** 592 (1970).
4. S. A. Akhmanov, R. V. Khokhlov, and A. P. Sukhorukov, in *Laser Handbook*, F. T. Arecchi and E. O. Schulz-Dubois, eds. (North-Holland, Amsterdam, 1972), Chap. E3.
5. For example, J. Gowar, *Optical Communications Systems* (Prentice-Hall, New York, 1983).
6. P. L. Baldeck, F. Raccah, and R. R. Alfano, Opt. Lett. **12,** 588 (1987).
7. A. Yariv, *Quantum Electronics* (Wiley, New York, 1975).
8. J. T. Manassah, M. A. Mustafa, R. R. Alfano, and P. P. Ho, IEEE J. Quantum Electron. **QE-22,** 197 (1986).
9. J. H. Marburger, Prog. Quantum Electron. **4,** 35 (1975).
10. H. Kogelnik, Appl. Opt. **4,** 1562 (1965).
11. P. K. Tien, J. P. Gordon, and J. R. Whinnery, Proc. IEEE **53,** 129 (1965).
12. R. H. Stolen and C. Lin, Phys. Rev. A **17,** 1448 (1978).